PHOTONICS Research

Direct generation of 3.17 mJ green pulses in a cavity-dumped Ho^{3+}-doped fiber laser at 543 nm

Tianran Li,[1,2,3] Ziyu Wang,[1,2] Jinhai Zou,[1,2] Jinfen Hong,[1,2] Qiujun Ruan,[1,2] Hang Wang,[1,2] Zhipeng Dong,[1,2] and Zhengqian Luo[1,2,3,4,*]

[1]Fujian Key Laboratory of Ultrafast Laser Technology and Applications, Xiamen University, Xiamen 361005, China
[2]Department of Electronic Engineering, Xiamen University, Xiamen 361005, China
[3]Shenzhen Research Institute of Xiamen University, Shenzhen 518129, China
[4]Innovation Laboratory for Sciences and Technologies of Energy Materials of Fujian Province (IKKEM), Xiamen 361005, China
*Corresponding author: zqluo@xmu.edu.cn

Received 6 September 2022; revised 28 December 2022; accepted 2 January 2023; posted 5 January 2023 (Doc. ID 474977); published 27 February 2023

High-energy pulsed lasers in the green spectral region are of tremendous interest for applications in space laser ranging, underwater detection, precise processing, and scientific research. Semiconductor pulsed lasers currently are difficult to access to the so-called "green gap," and high-energy green pulsed lasers still heavily rely on the nonlinear frequency conversion of near-IR lasers, precluding compact and low-cost green laser systems. Here, we address this challenge by demonstrating, for the first time to the best of our knowledge, millijoule-level green pulses generated directly from a fiber laser. The green pulsed fiber laser consists of a 450 nm pump laser diode, a Ho^{3+}-doped ZBLAN fiber, and a cavity-dumping module based on a visible wavelength acousto-optic modulator. Stable pulse operation in the cavity-dumping regime at 543 nm is observed with a tunable repetition rate in a large range of 100 Hz–3 MHz and a pulse duration of 72–116 ns. The maximum pulse energy of 3.17 mJ at 100 Hz is successfully achieved, which is three orders of magnitude higher than those of the rare-earth-doped fiber green lasers previously reported. This work provides a model for compact, high-efficiency, and high-energy visible fiber pulsed lasers.

https://doi.org/10.1364/PRJ.474977

1. INTRODUCTION

High-energy, short-pulse visible lasers have important applications in microscopy, medical diagnosis, laser displays, and underwater detection [1–3]. Visible semiconductor lasers have gained a lot of attention as extremely efficient and compact light sources, but are still under developed in the "green gap" wavelength of 500–550 nm. So far, the main technology for green pulsed lasers is the nonlinear frequency conversion (e.g., frequency doubling [4], sum frequency [5], and parametric process [6]) of near-IR fiber or solid-state lasers [7]. Although this technique has been capable of 1 kW-average-power, 1 J green pulse generation by frequency doubling [8], it usually suffers from system complexity, vibration sensitivity, and high cost. In contrast, the direct generation of green pulses from rare-earth-doped fiber lasers is preferred, because a green pulsed laser source can be compact, user friendly, with low cost, and maintenance free. Therefore, there is always motivation to develop green rare-earth-doped fiber pulsed lasers. Some special application scenarios, such as earth–moon ranging [9], urgently need this kind of high-energy green pulsed fiber laser with a relatively compact structure as the preferred light source.

The rare-earth-doped ZBLAN glass fiber is considered the ideal gain medium to directly generate a high-efficiency visible laser due to its low phonon energy in the absence of multiphoton relaxation [10–15]. Several kinds of rare-earth ions (Er^{3+} [16], Ho^{3+} [17–20], Pr^{3+} [21–23], and Tb^{3+} [24]) in fluoride fibers can be used for green emission. In recent years, with the rapid development of high-power blue GaN laser diodes (LDs), the frequency down-conversion green laser using Pr^{3+}-doped or Ho^{3+}-doped ZBLAN fibers has reached watt-level output power in CW operation [25,26]. Nakanishi *et al.* reported a 598 mW, 522.2 nm Pr^{3+}-doped fluoride single-clad fiber laser with a slope efficiency of 43% [23]. Most recently, Ji *et al.* used a 0.5% (molar fraction) Ho^{3+}-doped fluoroaluminate single-clad multimode fiber (30 cm long) to demonstrate watt-level laser emission in the green band [26]. Although a CW rare-earth-doped fiber laser operating at a green wavelength has been widely investigated, to the best of our knowledge, few reports on green pulsed fiber lasers have previously been published. Kojou *et al.* presented a 536–542 nm actively *Q*-switched Pr^{3+}-doped fiber laser with 4 μJ green pulse energy [27]. Luo *et al.* demonstrated a compact self-*Q*-switched up-conversion

Er:ZBLAN all-fiber laser operating at 543.4 nm [28]. In 2019, Li *et al.* reported a self-*Q*-switched Ho^{3+}:ZBLAN fiber to achieve 264 nJ green pulse at 550 nm [29]. However, one should notice that the green pulse energy from these *Q*-switched fiber lasers [27–29] is still limited to a relatively low level (less than a few microjoule), which could restrict such green pulsed fiber lasers to certain applications (e.g., earth–moon laser ranging [9]). Interestingly, it is well-known that cavity dumping is an excellent technique to achieve a laser pulse with the advantages of large pulse energy, a wide repetition-rate tuning range, and high efficiency [30,31]; however, until now, to the best of our knowledge, a cavity-dumped fiber laser in the visible region has not yet been reported.

In this paper, a high-energy cavity-dumped Ho^{3+}-doped ZBLAN fiber (Le Verre Fluoré) pulsed laser operating at ~543 nm is experimentally demonstrated for what we believe is the first time. A 450 nm LD was used to pump a high-concentration Ho^{3+}:ZBLAN fiber to provide green down-conversion gain, and a highly reflective mirror and a homemade fiber end-facet mirror at green wavelengths were employed to form the laser resonant cavity. Then, the green cavity dumping module is constructed by a visible-wavelength spatial modulator and a Z-type light feedback, which will support the completed oscillation of the first-order diffraction light and fully extract out the zeroth-order light. The laser directly generates a 317 mW, 543 nm green pulsed output with a repetition rate tuning from 100 Hz to 3 MHz and a slope efficiency of 55.3%. Stable cavity-dumped green pulses with a 116 ns duration could obtain a green pulse energy as high as 3.17 mJ at 100 Hz. Such a high-energy pulsed fiber green laser source could provide a new, promising light source for many applications in long-distance laser ranging, underwater detection, and microscopy.

Figure 1(a) shows the photograph and Fig. 1(b) shows the corresponding schematic of our proposed green cavity-dumped Ho^{3+}:ZBLAN fiber pulsed laser. The green laser consists of a 450 nm LD, an active fiber (Ho^{3+}:ZBLAN fiber), three highly reflective mirrors (M_1, M_3, and M_4), a fiber end-facet mirror (M_2), and a green spatial modulator. The 18 cm long Ho^{3+}:ZBLAN fiber (3000 parts per million by weight, a numerical aperture of 0.23, 7.5/125 μm core/cladding diameters) is used as gain medium and its absorption coefficient is about 2.9 dB/cm at 450 nm [32]. The 12 W, 450 nm LD as pump source is coupled to the gain fiber through a 7.5 mm focal-length aspherical lens (L_1) with a coupling efficiency of 11%. The green resonant cavity is constructed by the homemade fiber end-facet mirror (M_2) and the plane mirror (M_3). The fiber mirror M_2 is directly connected to the gain fiber by a standard FC/PC fiber adaptor. The mirror M_4 was used to extract the cavity-dumped light. All of them (M_2, M_3, and M_4) were coated with the same multilayer dielectric SiO_2/Ta_2O_5 films. The insets of Fig. 1(c) give the microscopic images of the fiber end-facet mirror M_2, indicating the good and uniform deposition of the multilayer films. The transmission spectrum of the three mirrors shown in Fig. 1(c) shows a high transmittance of >95% at 450 nm pump wavelength and a high reflectivity of >99.5% at a ~540 nm green oscillation wavelength. The highly reflective dichroic mirror (M_1) is rotated at a ~30° angle to input the pump light into the gain fiber and separate the green light into the spatial cavity-dumped module.

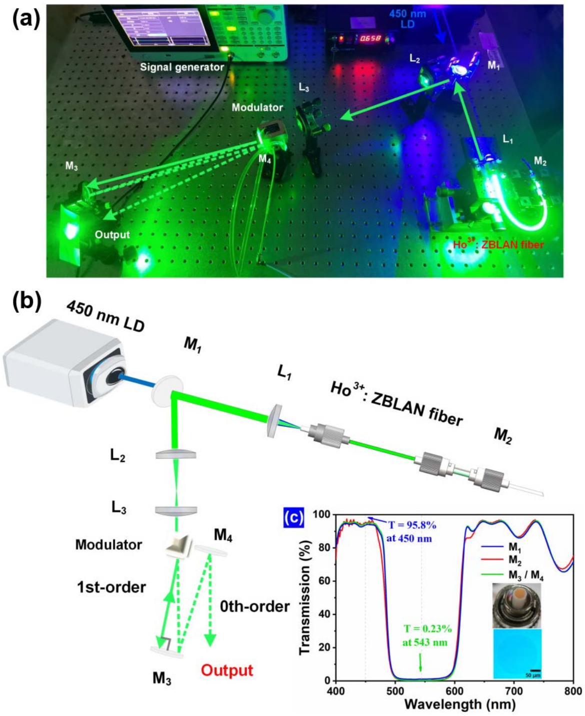

Fig. 1. (a) Photograph of green cavity-dumped Ho^{3+}-doped fiber laser. (b) Schematic of green cavity-dumped Ho^{3+}-doped fiber laser. (c) Optical transmission spectra of the visible-reflection mirror (M_1) at 30° deflection, fiber pigtail mirror (M_2), and visible-reflection mirrors (M_3, M_4), respectively.

2. EXPERIMENT SETUP AND OPERATION PRINCIPLE

The customized visible-wavelength spatial modulator is a key element for green cavity dumping. The visible spatial acousto-optic modulator with an RF operation frequency of 100 MHz can work in the wide visible range of 530–640 nm. The first-order diffraction efficiency at 540 nm is ~53%, and the insertion loss is 0.5 dB. A pair of plane-convex lenses (L_2 and L_3) is used to compress the green light beam into the modulator, and the switching rise and fall time can be as short as ~50 ns. In our experiment, the resonant cavity formed by M_3 and M_2 establishes a complete feedback of the first-order diffracted light, and the cavity-dumped pulses are extracted from the zeroth-order light by M_4. The operational principle of the green acousto-optic cavity dumping is described in Fig. 2. When a periodical electric signal, shown in Fig. 2(a), is used to modulate the cavity dumping system, the formation of cavity-dumped green laser pulses will experience the three stages shown in Fig. 2(b). (1) With the high-level electric signal, the first-order diffraction light is with high loss and the green laser cannot oscillate, so this stage is the energy storage phase. (2) With the low-level electric signal, the first-order diffraction light becomes low loss, and the green resonator completely oscillates without power output (owing to the full reflector M_3); therefore, in this stage the

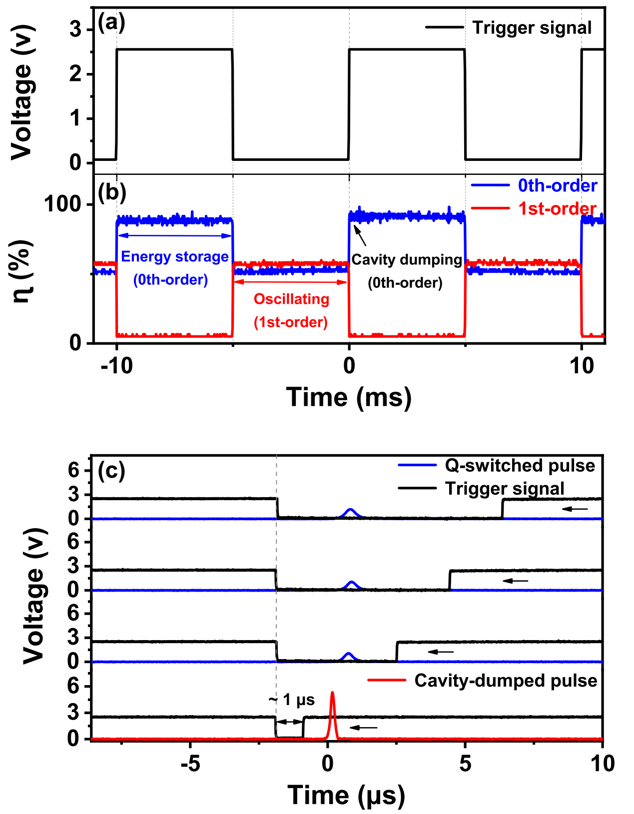

Fig. 2. (a) Periodical electric signal. (b) Formation of cavity-dumped green laser pulses and diffraction efficiency measurement at 543 nm of visible wavelength spatial modulator. (c) Process of generating cavity-dumping pulses by controlling the duty cycle of trigger signals.

green laser energy is fully stored in the cavity. (3) Finally, once the electric signal is quickly switched to a high level again, the intracavity green laser is instantaneously dumped by the zeroth-order light path, and therefore a high-energy green pulse can be achieved. After that, a new cycle can begin. In Fig. 2(c), to understand the mechanism of acousto-optic cavity dumping technology, we experimentally investigated the formation process of an acousto-optic cavity-dumped pulse by controlling the duty ratio of the electric signal. When the duty ratio is large (i.e., the low-voltage window is longer), the output pulse in the low-voltage window is a *Q*-switched pulse with low pulse energy. In contrast, when the duty ratio is small (i.e., the low-voltage level window is less than 1 μs), a very strong cavity-dumped pulse arising in the next high-voltage window can be clearly observed. This means that the device has a longer energy storage phase to get higher energy pulses at low repetition rates, as well as a wide range of repetition rate tunability. At the same time, considering that the pulse width is limited by the rise/fall time of the modulator, the duty cycle of the electrical signal is properly adjusted to ensure that the oscillation time in the cavity is several times longer than the rise/fall time to obtain a stable pulse output. The most important advantage is that this high-energy pulse can be extracted in a round trip time, independent of the time required to build up the power in the resonator cavity. Thus, the pulse width mainly depends on the length of the resonator when the switching time of the modulator does not exceed the round-trip time of the resonator.

In our experiment, the output performance of the green pulsed laser in the spectral and time domains is characterized by a 350–1750 nm optical spectrum analyzer (AQ-6315E, Ando) with a 0.05 nm resolution, an integrated-sphere power meter (S142C, Thorlabs), a photodetector (DET10A, Thorlabs), a digital oscilloscope (TDS1012C, Tektronix), and a radio frequency (RF) spectrum analyzer (GSP-930, Gwinstek).

3. EXPERIMENTAL RESULTS

A. High-Energy Green Pulse at 100 Hz

To verify the feasibility of high-energy green pulse generation, we output the green cavity-dumped fiber laser at a 100 Hz repetition rate. Figure 3 gives the output characteristics. Under a ∼20 cm Ho^{3+}:ZBLAN gain fiber, the green laser threshold is about 330 mW, and the green cavity-dumped pulses were clearly observed. The typical oscilloscope trace in the inset of Fig. 3(a) shows the stable pulse trains with a 10 ms period (i.e., 100 Hz repetition rate) and a pulse-to-pulse fluctuation as low as 5%. The pulse duration is 116 ns, and the single pulse envelope has a symmetric Gaussian-like intensity profile. As shown in Fig. 3(b), we also measured the output RF spectra of cavity-dumped pulses. The RF SNR is greater than 42 dB, and the wideband output RF spectrum [the inset of Fig. 3(b)] has no other frequency components or modulation, implying the good stability of the green cavity-dumped laser.

The green output spectra at a 1 mJ pulsed energy are shown in Fig. 3(c). The central wavelength locates at 543.02 nm and the 3 dB linewidth is as narrow as 0.12 nm. Furthermore, we optimized the length of the Ho^{3+}:ZBLAN fiber to improve the output efficiency of the green pulsed laser. As plotted in Fig. 3(d), under the different lengths of 16, 18, and 21 cm, the slope efficiency is 45.0%, 55.4%, and 42.8%, respectively, and the highest output power is 317 mW at the 100 Hz repetition rate, corresponding to pulse energy as high as 3.17 mJ. Although the output power is not a roll-off from Fig. 3(d), the increase of the output power is limited due to the thermal damage of the Ho^{3+}:ZBLAN fiber end facet (behind the L_1 lens). Under the low fiber coupling efficiency of the 450 nm pump laser, the residual pump power is high to accumulate the abundant thermal damage to the fluoride fiber end facet. The laser intensity distribution [see the inset of Fig. 3(d)] and M^2 factors of the generated green fiber laser beam were measured by a beam quality analyzer (WinCamD-UCD12, DataRay). The measured $M^2_{x,y}$ parameters are 4.41 and 4.31, respectively, indicating that the green fiber laser is in multimode operation. The multi-mode operation originates from the 9.9 V parameter of 7.5 μm core diameter of the Ho^{3+}:ZBLAN fiber at 543 nm.

Figure 4 presents the evolution of the optical spectrum and single pulse envelope as the output energy at the 100 Hz repetition rate varies. When the output power increased from 6 to 200 mW, the output spectrum of the green fiber laser was measured with a 0.05 nm resolution, as shown in Fig. 4(a). Although the cavity mirrors (M_1–M_3) for a high-*Q* cavity cover a wide reflection band from 500 to 590 nm, as shown in

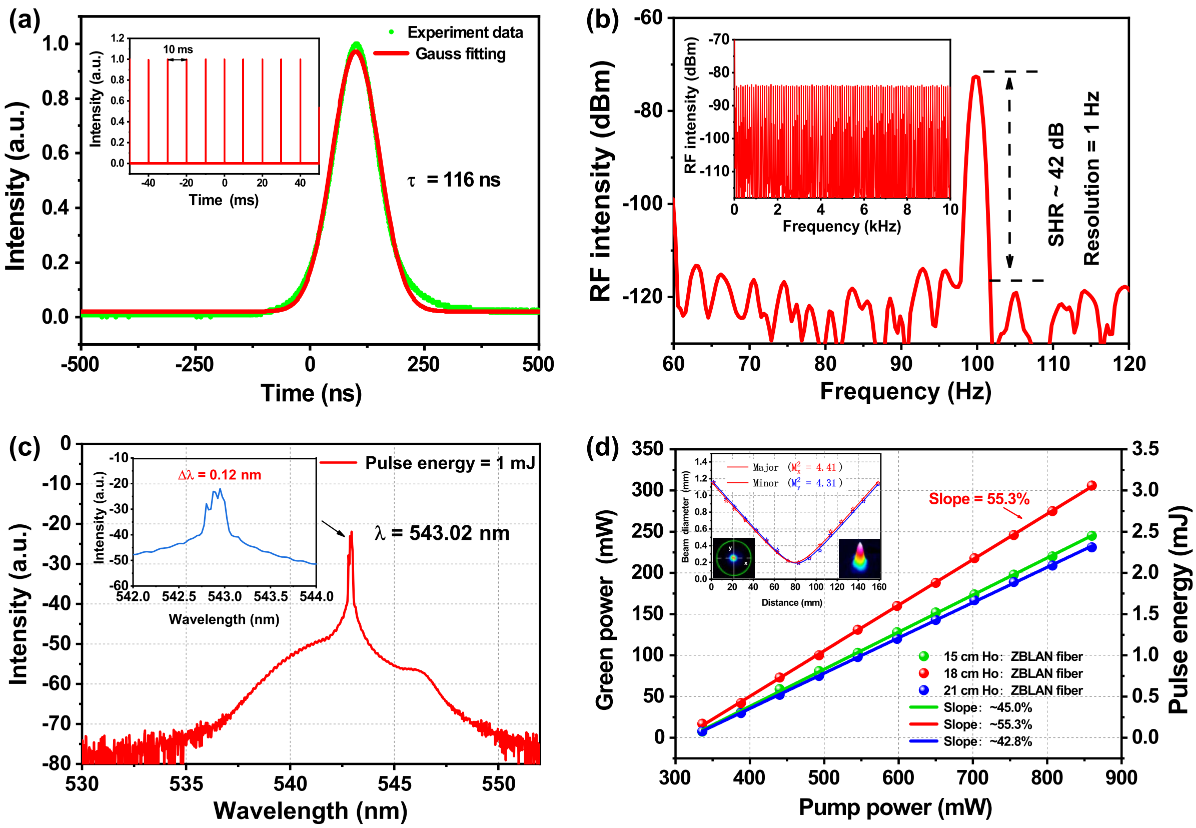

Fig. 3. Characteristics of the green cavity-dumped pulse operation at the millijoule energy level. (a) Single pulse. Inset: typical oscilloscope trace. (b) RF output spectra at 100 Hz. Inset: corresponding broadband RF output. (c) Output optical spectrum. Inset: close look at 543.02 nm. (d) Average output power as a function of the pump power envelope with gain fiber at different lengths. Inset: beam quality parameter and near-filed intensity distribution.

Fig. 1(c), the lasing occurs only at a single wavelength of ~543 nm without oscillating in multiple wavelengths. The central wavelength is always clamped at 543 nm and the 3 dB linewidth is less than 0.15 nm due to the filtering effect of acousto-optic Bragg diffraction in the process of the cavity-dumping operation.

Figure 4(b) shows the pulse profiles under the different pulse energies. It is clearly seen that the pulse profile remains almost unchanged (i.e., a Gaussian-like profile and 116 ns pulse duration). It should be attributed to the fact that the pulse duration in the cavity-dumped fiber laser is decoupled from the laser gain, resulting in the pulse duration at the same repetition rate being determined only by the resonator length. This means that in such green cavity-dumped Ho^{3+}-doped ZBLAN fiber lasers, even higher pulse repetition rates (such as a few MHz), narrower pulse duration (a few nanoseconds), and higher pulse energy are possible.

B. Repetition-Rate Tuning

A cavity-dumped laser is exceptionally steady for high pulse repetition rates (far above the inverse upper-state lifetime), because some light is always left in the laser resonator after pulse extraction and can serve as a seed for the next pulse. This means it is possible to obtain a very large pulse repetition rate tuning range based on the cavity-dumping technique. As shown in Fig. 5, the repetition rate tuning range can be from kilohertz to 3 MHz, and the pulse trains are stable with an intensity fluctuation as low as 5%. In our experiment, different repetition rates must satisfy the time conditions of energy storage and oscillation, so the electrical duty cycle must be fine-tuned slightly at different repetition rates.

Figure 6(a) gives the function of the green output power and pulse energy as the repetition rate at the fiber-coupling pump power of 0.85 W varies. Under the optimized 18 cm long gain fiber, the average output power (~310 mW) is almost constant in the case of a <7.1 kHz repetition rate, but the output power decreases when the repetition rate is over 7.1 kHz. The possible reason is that the time interval between two adjacent pulses (repetition rate >7.1 kHz) is less than the upper energy-level lifetime (~140 μs) of Ho^{3+}:ZBLAN fiber, so it does not get the maximum utilization of the population inversion. The corresponding pulse width and peak power at different repetition rates are shown in Fig. 6(b). As the repetition rate increased, the pulse width became short, and the ~70 ns shortest width is limited by the rise/fall time of the acousto-optic device. At the 3.17 mJ energy, we calculate the peak power precisely by integrating the pulse profile. The peak power is 24.6 kW at 100 Hz. To further enlarge the green pulse energy and compress the pulse width, a high-speed green acousto-optic spatial modulator with a smaller light beam size should be combined with a large-mode-area gain fiber.

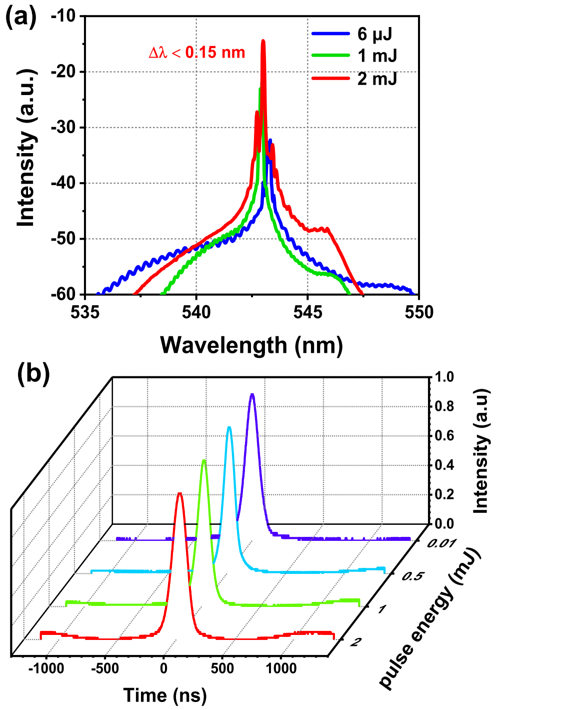

Fig. 4. (a) Output optical spectrum and (b) single pulse of the green cavity-dumped pulse under different pulsed energy.

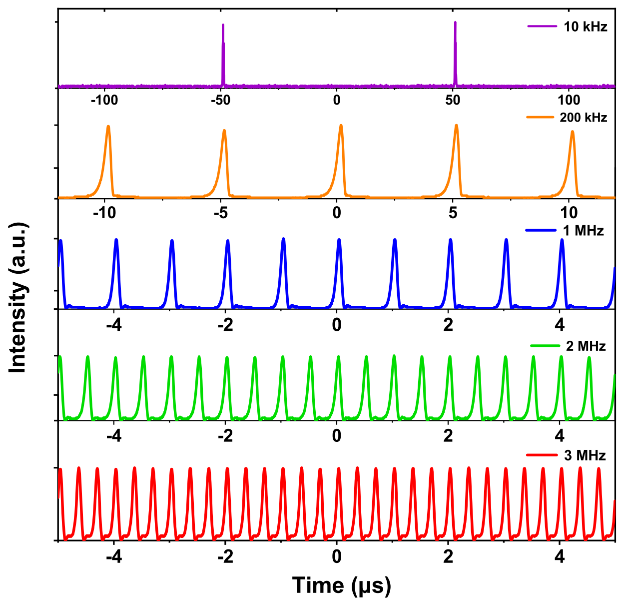

Fig. 5. Pulse trains based on cavity-dumping technology at different repetition rates.

To better illustrate the advantages of our green cavity-dumped fiber laser over other green fiber pulsed lasers previously reported, Table 1 compares the output performance of the typical rare-earth-doped pulsed fiber lasers operating at green wavelengths. Note that the previous techniques mostly used active *Q*-switching or passive *Q*-switching [17,27–29,34], but

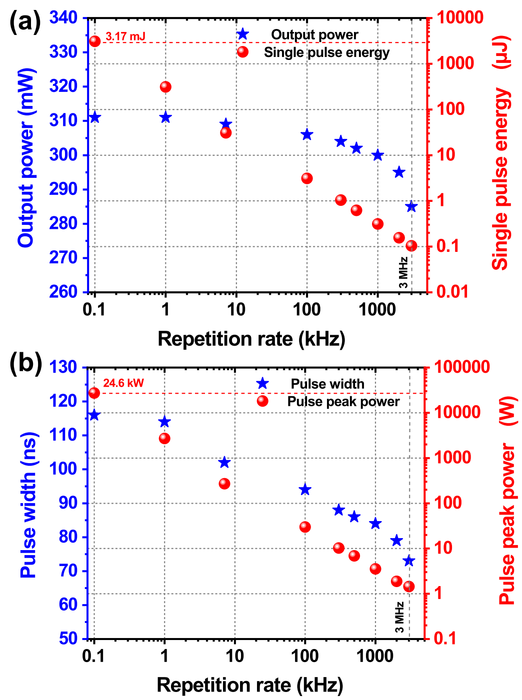

Fig. 6. Output characteristics of green cavity-dumped pulse at different repetition rate. (a) Corresponding average power and pulse energy at different repetition rates. (b) Corresponding pulse width and peak power at different repetition rates.

usually suffer from the restrictions, such as low pulse energy (only a few nJ or μJ), wide pulse duration (even μs), and narrow range (kHz) repetition rate. In this work, the cavity-dumping technique in a green fiber laser is exploited for the first time to significantly improve the output performance of green pulses. From Table 1 we can see that: (1) the green pulse energy is as high as 3.17 mJ at 543 nm, which is three orders of magnitude higher than previous reports [27–29], and (2) the repetition rate of our cavity-dumped green fiber laser can be tuned in a wide range of 0.1–3000 kHz, which is also two orders of magnitude larger than previous reports [27–29]. Moreover, the cavity-dumped green pulse has the shortest duration of 73 ns, which is also difficult to achieve by the nanosecond pulses previously reported based on *Q*-switching technology.

4. CONCLUSION

In summary, we have proposed and demonstrated a high-energy green cavity-dumped fiber laser at 543 nm. The green down-conversion gain was provided by a section of 18 cm high-concentration Ho^{3+}:ZBLAN fiber pumped by a 450 nm LD. The cavity dumping operation is accomplished by employing a visible-wavelength spatial modulator and designing the resonant cavity. The 3.17 mJ green pulses are directly generated, which is typically three orders of magnitude higher than that of a conventional *Q*-switched fiber laser. Moreover, the pulse repetition rate of the green cavity-dumped fiber laser can be widely tuned in a range of 100 Hz–3 MHz. This cavity-dumped green fiber laser is an important step toward

Table 1. Performance Comparison of Rare-Earth-Doped Pulsed Fiber Lasers at Green Wavelengths

Rare-Earth Ion	Operation Regime	Wavelength (nm)	Maximum Pulse Energy (μJ)	Repetition Rate (kHz)	Pulse Duration (ns)	Reference
Pr^{3+}	AO-*Q*-switch	520–526 536–542	1.99 4.16	8.3	160 298	[27]
Er^{3+}	Self-*Q*-switch	543.4	0.138	25.9–50.8	1950	[28]
	Passive *Q*-switch	543	0.0252	42.61–181.2	490–1990	[33]
Ho^{3+}	Self-pulsing	539–550	/	100	1000	[17]
	Self-*Q*-switch	550	0.264	58.61–70.59	889	[29]
	Cavity-dumping	**543**	**3170**	**0.1–3000**	**73–116**	**This work**

compact, large pulse energy, and high-efficiency pulse laser systems in the visible spectrum.

Funding. National Science Funds for Excellent Young Scholars (62022069); Shenzhen Science and Technology Projects (JCYJ20210324115813037); National Natural Science Foundation of China (62105272); Technology Development Program from Huawei Technologies Co., Ltd.; Fundamental Research Funds for the Central Universities (20720200068).

Disclosures. The authors declare no conflicts of interest.

Data Availability. Data underlying the results presented in this paper are not publicly available at this time but may be obtained from the authors upon reasonable request.

REFERENCES

1. J. A. Conchello and J. W. Lichtman, "Optical sectioning microscopy," Nat. Methods **2**, 920–931 (2005).
2. C. Framme, G. Schuele, J. Roider, R. Birngruber, and R. Brinkmann, "Influence of pulse duration and pulse number in selective RPE laser treatment," Lasers Surg. Med. **34**, 206–215 (2004).
3. Y. Fujimoto, J. Nakanishi, T. Yamada, O. Ishii, and M. Yamazaki, "Visible fiber lasers excited by GaN laser diodes," Prog. Quantum Electron. **37**, 185–214 (2013).
4. A. Liu, M. A. Norsen, and R. D. Mead, "60-W green output by frequency doubling of a polarized Yb-doped fiber laser," Opt. Lett. **30**, 67–69 (2005).
5. D. Taverner, P. Britton, P. G. R. Smith, D. J. Richardson, G. W. Ross, and D. C. Hanna, "Highly efficient second-harmonic and sum-frequency generation of nanosecond pulses in a cascaded erbium-doped fiber periodically poled lithium niobate source," Opt. Lett. **23**, 162–164 (1998).
6. Y. Y. Lin, R. Y. Tu, T. D. Wang, S. T. Lin, and Y. C. Huang, "Fiber-laser-pumped CW OPO for red, green, blue laser generation," Opt. Express **18**, 2361–2367 (2010).
7. I. Hong, K. Lee, and J. H. Lee, "532-nm second harmonic generation with enhanced efficiency using subharmonic cavity modulation-based quasi-*Q*-switched-mode-locked pulses," Opt. Express **28**, 25431–25443 (2020).
8. H. Chi, Y. Wang, A. Davenport, C. Menoni, and J. Rocca, "Demonstration of a kilowatt average power, 1 J, green laser," Opt. Lett. **45**, 6803–6806 (2020).
9. G. Martinot-Lagarde, M. Aimar, D. Albanèse, C. Courde, and H. Viot, "Laser enhancements for lunar laser ranging at 532 nm," Results Phys. **6**, 329–336 (2016).
10. S. Ji, Y. Song, Z. Wang, C. Shen, J. Lin, B. Xiao, Q. Feng, Q. Du, H. Xu, and Z. Cai, "High power downconversion deep-red emission from Ho^{3+}-doped fiber lasers," Nanophotonics **11**, 1603–1609 (2022).
11. J. Zou, T. Li, Y. Dou, J. Li, N. Chen, Y. Bu, and Z. Luo, "Direct generation of Watt-level yellow Dy^{3+}-doped fiber laser," Photon. Res. **9**, 446–451 (2021).
12. M.-P. Lord, V. Fortin, F. Maes, L. Talbot, M. Bernier, and R. Vallée, "2.3 W monolithic fiber laser operating in the visible," Opt. Lett. **46**, 2392–2395 (2021).
13. Q. Ruan, X. Xiao, J. Zou, H. Wang, S. Fan, T. Li, J. Li, Z. Dong, Z. Cai, and Z. Luo, "Visible-wavelength spatiotemporal mode-locked fiber laser delivering 9 ps, 4 nJ pulses at 635 nm," Laser Photon. Rev. **16**, 2100678 (2022).
14. S. Luo, H. Gu, X. Tang, X. Geng, L. Li, and Z. Cai, "High-power yellow DSR pulses generated from a mode-locked Dy:ZBLAN fiber laser," Opt. Lett. **47**, 1157–1160 (2022).
15. J. Zou, C. Dong, H. Wang, T. Du, and Z. Luo, "Towards visible-wavelength passively mode-locked lasers in all-fibre format," Light Sci. Appl. **9**, 1 (2020).
16. J. Y. Allain, M. Monerie, and H. Poignant, "Tunable green upconversion erbium fibre laser," Electron. Lett. **28**, 111–113 (1992).
17. D. Funk, S. Stevens, S. Wu, and J. Eden, "Tuning, temporal, and spectral characteristics of the green ($\lambda = 549$ nm), holmium-doped fluorozirconate glass fiber laser," IEEE J. Quantum Electron. **32**, 638–645 (1996).
18. W. Li, J. Wu, X. Guan, Z. Zhou, H. Xu, Z. Luo, and Z. Cai, "Efficient continuous-wave and short-pulse Ho^{3+}-doped fluorozirconate glass all-fiber lasers operating in the visible spectral range," Nanoscale **10**, 5272–5279 (2018).
19. D. Funk and J. Eden, "Laser diode-pumped holmium-doped fluorozirconate glass fiber laser in the green ($\lambda = 544$–549 nm): power conversion efficiency, pump acceptance bandwidth, and excited-state kinetics," IEEE J. Quantum Electron. **37**, 980–992 (2001).
20. J. Y. Allain and M. Monerie, "Room temperature CW tunable green upconversion holmium fibre laser," Electron. Lett. **26**, 261–263 (1990).
21. O. Hellmig, S. Salewski, A. Stark, J. Schwenke, P. E. Toschek, K. Sengstock, and V. M. Baev, "Multicolor diode-pumped upconversion fiber laser," Opt. Lett. **35**, 2263–2265 (2010).
22. H. Okamoto, K. Kasuga, and Y. Kubota, "Efficient 521 nm all-fiber laser: splicing Pr^{3+}-doped ZBLAN fiber to end-coated silica fiber," Opt. Lett. **36**, 1470–1472 (2011).
23. J. Nakanishi, Y. Horiuchi, T. Yamada, O. Ishii, M. Yamazaki, M. Yoshida, and Y. Fujimoto, "High-power direct green laser oscillation of 598 mW in Pr^{3+}-doped waterproof fluoroaluminate glass fiber excited by two-polarization-combined GaN laser diodes," Opt. Lett. **36**, 1836–1838 (2011).
24. T. Yamashita, G. Qin, T. Suzuki, and Y. Ohishi, "A new green fiber laser using terbium-doped fluoride fiber," in *Conference on Optical Fiber Communication/National Fiber Optic Engineers Conference*, OSA Technical Digest (CD) (Optica Publishing Group, 2008), paper JWA18.
25. J. Zou, J. Hong, Z. Zhao, Q. Li, Q. Ruan, H. Wang, Y. Bu, X. Guan, M. Zhou, Z. Feng, and Z. Luo, "3.6 W compact all-fiber Pr^{3+}-doped green laser at 521 nm," Adv. Photon. **4**, 056001 (2022).
26. S. Ji, S. Liu, X. Lin, Y. Song, B. Xiao, Q. Feng, W. Li, H. Xu, and Z. Cai, "Watt-level visible continuous-wave upconversion fiber lasers toward the "green gap" wavelengths of 535–553 nm," ACS Photon. **8**, 2311–2319 (2021).
27. J. Kojou, Y. Watanabe, P. Agrawal, T. Kamimura, and F. Kannari, "Wavelength tunable *Q*-switch laser in visible region with Pr^{3+}-doped fluoride-glass fiber pumped by GaN diode laser," Opt. Commun. **290**, 136–140 (2013).

28. Z. Luo, Q. Ruan, Z. Min, Y. Cheng, and Z. Cai, "Compact self-*Q*-switched green upconversion Er:ZBLAN all-fiber laser operating at 543.4 nm," Opt. Lett. **41**, 2258–2261 (2016).
29. W. Li, J. Wu, Z. Cai, X. Guan, and H. Xu, "Directly blue diode-pumped green self-*Q*-switched Ho^{3+}-doped fluoride all-fiber laser at 550 nm," J. Lightwave. Technol. **37**, 5727–5732 (2019).
30. D. Maydan and R. B. Chesler, "*Q*-switching and cavity dumping of Nd: YAIG lasers," J. Appl. Phys. **42**, 1031–1034 (1971).
31. I. Abdulhalim, C. N. Pannell, K. P. Jedrzejewski, and E. R. Taylor, "Cavity dumping of neodymium-doped fibre lasers using acousto-optic modulator," Opt. Quantum Electron. **26**, 997–1001 (1994).
32. J. Zou, J. Li, T. Li, Y. Huang, Q. Ruan, Y. Dou, and Z. Luo, "Tunable, continuous-wave, deep-ultraviolet laser generation by intracavity frequency doubling of visible fiber lasers," J. Lightwave Technol. **40**, 3900–3906 (2022).
33. J. Zou, Z. Kang, R. Wang, H. Wang, and Z. Luo, "Green/red pulsed vortex-beam oscillations in all-fiber lasers with visible-resonance gold nanorods," Nanoscale **11**, 15991–16000 (2019).
34. B. Guo, Q. Xiao, S. H. Wang, and H. Zhang, "2D layered materials: synthesis, nonlinear optical properties, and device applications," Laser Photon. Rev. **13**, 1800327 (2019).